

Accelerating Diffusion Transformer via Error-Optimized Cache

Junxiang Qiu¹ Shuo Wang¹ Jinda Lu¹ Lin Liu¹ Houcheng Jiang¹ Yanbin Hao²

Abstract

Diffusion Transformer (DiT) is a crucial method for content generation. However, it needs a lot of time to sample. Many studies have attempted to use caching to reduce the time consumption of sampling. Existing caching methods accelerate generation by reusing DiT features from the previous time step and skipping calculations in the next, but they tend to locate and cache low-error modules without focusing on reducing caching-induced errors, resulting in a sharp decline in generated content quality when increasing caching intensity. To solve this problem, we propose the Error-Optimized Cache (EOC). This method introduces three key improvements: (1) Prior knowledge extraction: Extract and process the caching differences; (2) A judgment method for cache optimization: Determine whether certain caching steps need to be optimized; (3) Cache optimization: reduce caching errors. Experiments show that this algorithm significantly reduces the error accumulation caused by caching (especially over-caching). On the ImageNet dataset, without significantly increasing the computational burden, this method improves the quality of the generated images under the over-caching, rule-based, and training-based methods. Specifically, the Fréchet Inception Distance (FID) values are improved as follows: $6.857 \rightarrow 5.821$, $3.870 \rightarrow 3.692$ and $3.539 \rightarrow 3.451$ respectively.

1. Introduction

Content generation aims to automatically produce text (Achiam et al., 2023), images (Xu et al., 2024), videos (Wang et al., 2024), and other forms of content based on existing data or context. It is widely used in intelligent customer service dialogue generation, news summarization, and advertising copy creation. However, current genera-

¹University of Science and Technology of China, Hefei, China
²Hefei University of Technology, Hefei, China. Correspondence to: Shuo Wang <shuowang.edu@gmail.com>.

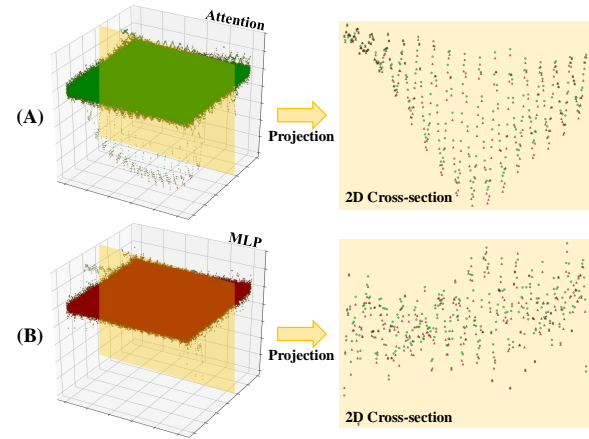


Figure 1. The adjacent steps' outputs of (A) Attention and (B) MLP layers during the DiT calculation.

tion methods often rely on complex models, resulting in cumbersome and time-consuming computational processes that hinder rapid deployment and flexible application in real-world business contexts. Therefore, accelerating content generation to enhance model inference efficiency and scalability is a critical challenge.

Recent approaches often employ strategies like pruning (Liu et al., 2018) or caching (Ma et al., 2024b) to accelerate generative processes and tackle inference-speed and scalability challenges. Unlike pruning (removing unimportant parameters/neurons to simplify the model), caching methods can reuse intermediate computation results across multiple sampling or inference steps. This greatly boosts inference efficiency while preserving the model's expressive capacity. Common caching strategies fall into two broad types: rule-based (Selvaraju et al., 2024), analyzing generated-content variations during sampling to decide what to cache/skip, and training-based (Ma et al., 2024a), enabling the model to automatically learn when, where, and how to cache/skip unimportant computational modules. These strategies are often integrated into the Diffusion Transformer (DiT) (Peebles & Xie, 2023) model as the DiT has robust learning capabilities and maintains data dimensions during sampling, facilitating easy validation of these acceleration strategies.

However, the caching-based DiT method typically reuses the same computational blocks across consecutive steps without

Table 1. Effects of No Cache, Light Cache, and Excessive Cache.

Method	Reused	IS \uparrow	FID \downarrow	sFID \downarrow
No Cache	0%	223.49	3.484	4.892
Cache	25%	220.01	3.87	5.19
	50%	190.05	6.86	8.76

sufficiently analyzing potential errors in the cached content, leading to cumulative errors at each caching operation. To verify this, we visualize the outputs of the Attention and MLP layers from the DiT computation process in Figures 1(A) and 1(B), focusing on the same blocks in adjacent steps. Specifically, the red dots represent the previous step, while the green dots correspond to the current step. Although most points from these two steps lie on a shared hyperplane, numerous outliers exhibit substantial deviations. We project one layer into a 3D structural diagram to further illustrate these discrepancies. We can find that even within that hyperplane, there are discernible gaps between the two point sets. Thus, in conventional DiT methods, the caching process typically begins by statistically analyzing how caching specific modules affects generation quality, aiming to identify those with minimal impact. The method then replaces the current step’s outputs (green) with those from the previous step (red) to reduce computation. However, this replacement process disregards the underlying differences, amplifying errors through repeated reuse. Additionally, the absence of thorough error analysis requires careful selection of which modules to cache. Over-caching can severely degrade both the quality and stability of the generated content. As shown in Table 1, we further validated these observations using a rule-based DiT method (Selvaraju et al., 2024) and tested caching at 0%, 25%, and 50%. While caching 25% of the blocks yields results comparable to those without caching, caching 50% of the blocks noticeably degrades generation quality. This decline occurs because blocks with large errors, once cached, accumulate and manifest as noise or extraneous artifacts, ultimately compromising the overall quality of the generated content.

Inspired by the concept of knowledge editing (Meng et al., 2022), we propose introducing different values from corresponding positions in prior knowledge to mitigate significant caching errors, thereby reducing the negative impacts of caching. Prior knowledge refers to the outputs of the attention layer and the MLP layer of each DiT block at every step of the sampling process. Specifically, we begin by determining which caching modules require optimization, measuring two factors: (1) the magnitude of error introduced when caching a given module, and (2) the relative position of that module’s step in the overall sampling process. Larger errors, especially if they occur early in sampling, are more prone to accumulation. By weighting and summing these two factors, we derive an indicator to identify modules that demand

caching optimization. Once such modules are identified, we introduce controlled perturbations into the cached content during sampling to further reduce errors. Specifically, when a module is selected for caching, we calculate the “trend” at the same position in the prior knowledge and embed it into the caching operation via weighted multiplication. This effectively maps the prior knowledge’s trend to the sampled data, helping to maintain the stability and quality of the generated results while benefiting from the computational efficiency of caching.

In summary, the contributions of Error-Optimized Cache (EOC) are threefolds:

- We design a module that extracts and processes the model’s operational data, capturing the characteristics of changes between blocks. It can be reused in different caching methods under the same model.
- We propose a method that determines when caching steps require optimization. This ensures sufficient optimization and prevents over-optimization of caching from causing blurring of details.
- Our approach reduces caching errors, enhances the robustness of cached models and raises the upper bound on image generation speed without sacrificing quality.

2. Related Work

In this section, we review existing diffusion acceleration methods and outline the differences between our proposed EOC approach and these related techniques.

2.1. Traditional generation acceleration

Common methods for sampling acceleration include pruning, quantization, and sampling method optimization.

Model Pruning And Quantization. Pruning reduces model complexity and computational cost by removing less critical weights, neurons, or layers while maintaining performance. It involves unstructured pruning (Dong et al., 2017; Lee et al., 2019), which masks individual parameters, and structural pruning (Liu et al., 2021), which removes larger components like layers or filters. In diffusion models, techniques like LD-Pruner (Castells et al., 2024) and DiffPruning (Guo et al., 2020) enhance efficiency by applying structured pruning and using informative gradients to reduce unnecessary steps and weights.

Quantization lowers the precision of weights and activations to smaller bit formats, reducing model size and speeding up inference. Key methods include Quantization-Aware Training (QAT) (Bhalgat et al., 2020) and the more efficient Post-Training Quantization (PTQ) (Li et al., 2021; Nagel et al., 2020), which doesn’t require retraining. For diffusion

models, PTQ methods such as PTQ4DiT (Wu et al., 2024) and Q-diffusion (Li et al., 2023b) optimize activation variance across denoising steps, while TDQ (So et al., 2024) uses MLP layers for step-wise parameter estimation. These approaches aim to balance performance with efficiency.

Sampling Method Optimization. Sampling method optimization for diffusion models aims to reduce generation time while maintaining sample quality. These can be categorized into re-training methods, like knowledge distillation (Luhman & Luhman, 2021; Salimans & Ho, 2022), and those that do not require re-training, such as advanced samplers for pre-trained models. Notably, DDIM (Song et al., 2020) reduces sampling steps using non-Markovian processes, while DPM-Solver (Lu et al., 2022) leverages ODE solvers. Progressive distillation (Meng et al., 2023; Yin et al., 2024), consistency models (Song et al., 2023), and parallel sampling methods like DSNO (Zheng et al., 2023) and ParaDiGMS (Shih et al., 2024) also enhance efficiency without additional training, making diffusion models more practical for real-world applications.

2.2. Caching Method

In addition to the methods mentioned above, caching offers another low-cost and highly adaptable approach to accelerate generation. Initially, Faster Diffusion (Li et al., 2023a) and DeepCache (Ma et al., 2024b) observed the sampling process to cache and reuse module outputs with minimal loss. Cache-Me-if-You-Can (Wimbauer et al., 2024) uses a teacher-student model to mimic the original model’s sampling process, reducing caching errors. However, these techniques are designed for U-Net-based models (Song et al., 2020) and are difficult to apply directly to DiT-based models (Peebles & Xie, 2023).

Next, Fora (Selvaraju et al., 2024) implemented a caching mechanism that stores and reuses intermediate outputs of attention and MLP layers across denoising steps, reducing computational overhead. Δ -DiT (Chen et al., 2024) uses a designed caching mechanism to accelerate the later DiT blocks in the early sampling stages and the earlier DiT blocks in the later stages. These works extend caching to DiT-based models. PAB (Zhao et al., 2024) reduces redundancy by utilizing a U-shaped attention pattern in the diffusion process and expands caching to video generation through pyramid broadcasting. Beyond the rule-based methods mentioned, learning-to-cache (Ma et al., 2024a) achieves higher acceleration by using a learnable router to decide whether each layer needs computation, though it incurs significant computational costs.

Differences: The above methods focus more on identifying the less important (cacheable) parts of the model using different approaches, thereby balancing generation speed and quality. They lack consideration of errors in the cached

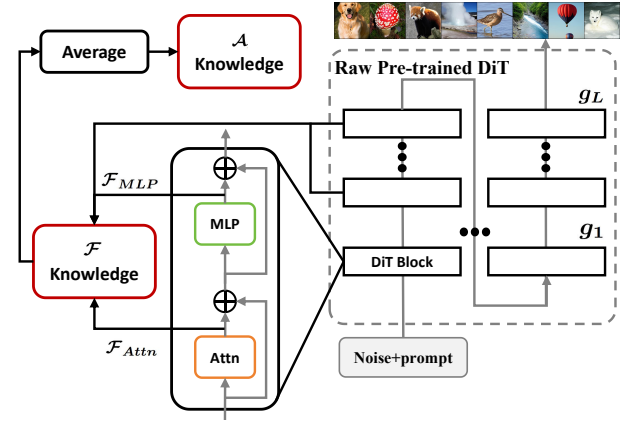


Figure 2. Prior Knowledge Extraction. We input different prompts multiple times for sampling and record the outputs of the Attention and MLP layers.

content. In contrast, the EOC method proposed in this paper maximizes the reduction of error accumulation caused by cache errors. It can be applied to both rule-based and training-based methods.

3. Method

In this section, we first introduce our work by presenting the DiT and Cache methods. Subsequently, we elaborate on the three main steps encompassed in EOC: (1) Prior Knowledge Extraction (PKE, Figure 2); (2) Cache Optimization Determination (COD, yellow side of Figure 3); (3) Cache Optimization (CO, blue side of Figure 3).

3.1. Preliminaries

Diffusion Models. Diffusion models (Ho et al., 2020) contain: (1) The forward process: By gradually adding Gaussian noise, the original image x_0 is added with noise to become the random noise x_t ; (2) The reverse process: The Gaussian random noise x_t is gradually denoised to reconstruct the original image x_0 . To achieve the step-by-step process, the model needs to learn the inverse process of noise addition. Therefore, we can model the reverse process $p_{\theta}(x_{t-1} | x_t)$ using Markov chains \mathcal{N} as follows:

$$\mathcal{N}\left(x_{t-1}; \frac{1}{\sqrt{\alpha_t}} \left(x_t - \frac{1 - \alpha_t}{\sqrt{1 - \alpha_t}} \epsilon_{\theta}(x_t, t)\right)\right), \quad (1)$$

in which t represents the denoising step, β_t represents the noise variance schedule. $\alpha_t = 1 - \beta_t$, $\bar{\alpha}_t = \prod_{i=1}^t \alpha_i$, and T represents the total number of denoising steps. And ϵ_{θ} is a deep network parameterized by θ . It takes x_t as input and outputs a prediction of the noise required for the denoising process. During the generation procedure with T timesteps, ϵ_{θ} is employed for inference T times. This

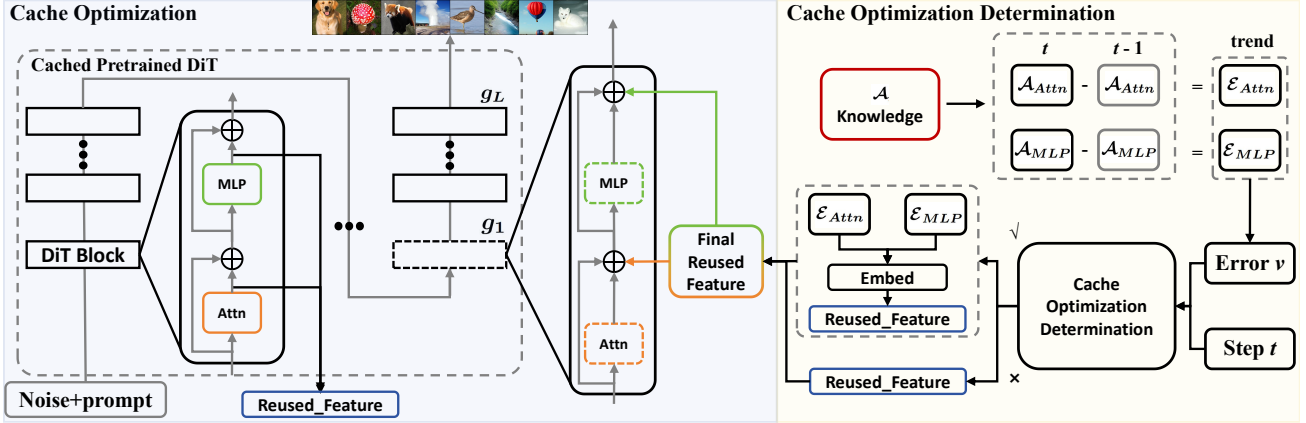


Figure 3. Pipeline of EOC after extracting prior knowledge. Cache Optimization Determination: Based on the information from adjacent steps, decide whether to perform cache optimization at the current step and calculate the final reused feature; Cache Optimization: Add the processed final reused features into the caching process to reduce cache errors.

repeated inference is what incurs the major computational costs in diffusion models.

Diffusion Transformer. Diffusion Transformer (DiT) (Peebles & Xie, 2023), typically consists of stacked groups of attention layer \mathcal{F}_{Attn} and multilayer perceptron \mathcal{F}_{MLP} . Mathematically, it can be approximately described by the following formulation:

$$\begin{aligned} \mathcal{G} &= g_1 \circ g_2 \circ \dots \circ g_L, \quad \text{where} \\ g_l &= \mathcal{F}_{Attn}^l \circ \mathcal{F}_{MLP}^l, \end{aligned} \quad (2)$$

in which \mathcal{G} represents the overall DiT model, g_l stands for the individual blocks within the DiT architecture, and \mathcal{F}^l denotes the different layers in a single DiT block. The computational output dimensions of these modules and layers are all the same. The variable l serves as the index for the DiT blocks, while L represents the depth of the DiT model. Before delving into the general computation between \mathcal{F} and \mathbf{x} , it's essential to introduce AdaLN (Guo et al., 2022), referring to the adaptive layer normalization. It has become an important component in modern neural network architectures, especially in the context of DiT. Subsequently, the general computation between \mathcal{F} and \mathbf{x} can be written as:

$$\begin{aligned} \mathcal{F}_{Attn} &= \mathbf{x} + \text{AdaLN} \circ \mathbf{f}_{Attn}(\mathbf{x}), \\ \mathcal{F}_{MLP} &= \mathbf{x} + \text{AdaLN} \circ \mathbf{f}_{MLP}(\mathbf{x}), \end{aligned} \quad (3)$$

in which, \mathbf{x} represents the residual connection and \mathbf{f} represents either the MLP or the attention layers. Here, AdaLN is applied to the outputs of $\mathbf{f}_{Attn}(\mathbf{x})$ and $\mathbf{f}_{MLP}(\mathbf{x})$. By normalizing these values adaptively, AdaLN helps to stabilize the training process, improve the model's generalization ability, and enhance the overall performance of the DiT model in handling complex data patterns.

Feature Caching. Feature caching is centered on the principle of re-utilizing features that were calculated and stored during earlier timesteps. The primary objective is to avoid redundant computations in the subsequent timesteps. This caching mechanism generally operates through multiple, repeated caching intervals. Let's assume there is a caching interval that encompasses N timesteps, starting from timestep t and ending at timestep $t + N - 1$. In this scenario, during timestep t , feature caching performs a full-fledged calculation and then stores the generated features. Symbolically, we can represent this process as $\mathcal{C}[l] := g_l(\mathbf{x}_t)$. Here, \mathcal{C} denotes the cache, $g_l(\mathbf{x}_t)$ corresponds to the output of the attention layer \mathcal{F}_{Attn} and the multilayer perceptron \mathcal{F}_{MLP} of the l -th block at the t -th timestep, and the symbol “:=” represents an assignment operation. After that, for the timesteps from $t+1$ to $t+N-1$, instead of carrying out new computations, the system leverages the pre-stored features. Mathematically, this can be formulated as $g_l(\mathbf{x}_{t+i}) := \mathcal{C}[l]$, where i is a non-negative integer and $i \leq N - 1$.

3.2. Error-Optimized Cache

For Feature Cache, previous work has centered on using different methods to locate modules that are either irrelevant or weakly related to sampling for caching, thus accelerating the generation process. However, they lack an exploration of caching errors. As a result, all these methods have a relatively low acceleration ceiling. Therefore, we aim to introduce low-cost prior knowledge with almost no time cost, to offset the relatively large caching errors to the greatest extent. As shown in Figure 2, to achieve this goal, first, we need to obtain the targeted output trends of each block through a large number of pre-sampling. And as shown in Figure 3, we need to determine whether a module to be cached requires optimization. Finally, we also need to em-

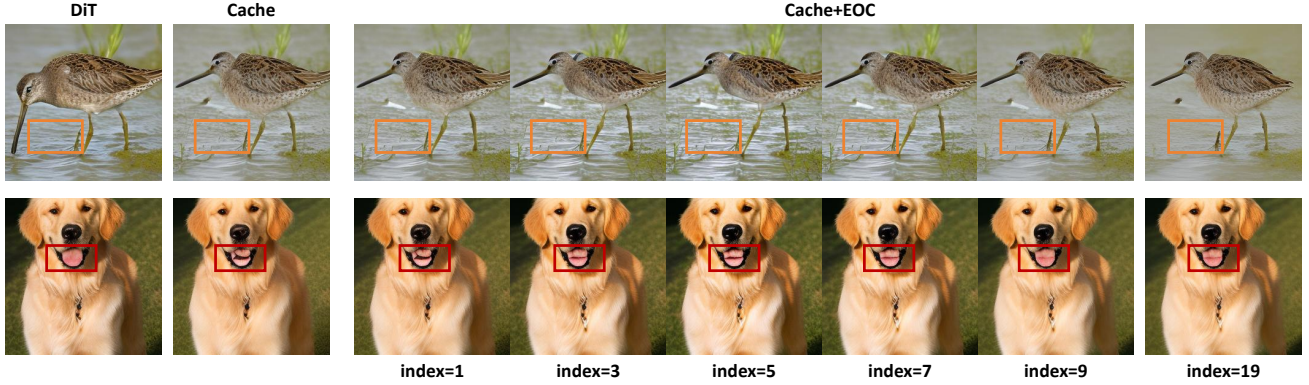


Figure 4. Effect of COD. The generation quality after performing CO on cached blocks with $t \leq index$.

bed this prior information into the sampling process. Next, we will introduce these three methods in detail.

Prior Knowledge Extraction. In order to determine whether to perform cache optimization and carry out such optimization in subsequent work, we need to record every output $g(x)$ of the model during the sampling process. Specifically, we will use classes that cover all categories or as many prompts as possible. These will be input into the model separately and multiple times for original generation without caching. As shown in Figure 2, during each generation process, we will add hooks to record the outputs $\mathcal{F}_{\text{Attn}}$ and \mathcal{F}_{MLP} of the Attention layers and MLP layers in all blocks of the DiT model after calculation. Subsequently, we will calculate the average of the Attention and MLP outputs at each position respectively, so as to obtain representative features $\mathcal{A}_{\text{Attn}}$ and \mathcal{A}_{MLP} of the model generation process. Assuming that the sampling is performed Q times and q represents the specific sampling number. The specific calculation functions are shown as follows:

$$\begin{aligned} \mathcal{A}_{\text{Attn}} &= \frac{1}{Q} \sum_{q=1}^Q \mathcal{F}_{\text{Attn}}^q, \\ \mathcal{A}_{\text{MLP}} &= \frac{1}{Q} \sum_{q=1}^Q \mathcal{F}_{\text{MLP}}^q. \end{aligned} \quad (4)$$

Cache Optimization Determination. To determine whether a block to be cached requires cache optimization, we believe that two points need to be focused on: (1) If caching a certain block has a significant negative impact on the model, or in other words, if the output of the block whose calculation is to be skipped differs greatly from the output of the block whose cache is to be reused, then we will prioritize the optimization of these caches. (2) If cache optimization is performed on a block, and the embedded optimized content will lead to wrong details or blurred background in the model output, then we will avoid optimizing

these caches.

First, we analyze the prior knowledge extracted in the previous part. In the previous step (the $(t-1)$ -th step) and subsequent (the t -th step) steps, the blocks at the same position can be regarded as the modules to be calculated, cached, and reused, and the modules to be skipped, respectively. Therefore, by calculating the differences of the corresponding modules, we can obtain the change trend of each pixel point, which is collectively referred to as "trend", namely $\mathcal{E}_{\text{Attn}}$ and \mathcal{E}_{MLP} . The specific calculation functions are shown as follows:

$$\mathcal{E}_{(t,l)} = \mathcal{A}_{(t,l)} - \mathcal{A}_{(t-1,l)} \in \mathbb{R}^{j \times k} \text{ when } t \neq 0, \quad (5)$$

in which, j and k are the same dimensions of \mathcal{F} , \mathcal{A} and \mathcal{E} . For the "trends" $\mathcal{E}_{\text{Attn}}$ and $\mathcal{E}_{\text{MLP}} \in \mathbb{R}^{j \times k}$, we calculate the average value \mathcal{V} of all the $j \times k$ pixel points after taking their absolute values. A larger average value \mathcal{V} indicates a greater error between the corresponding modules. And we will prioritize the cache optimization for the modules with larger \mathcal{V} values.

Next, through observation, the absolute values of each pixel value in the trend vary. For relatively large values, we believe that they are the accumulation of many numbers with the same sign (positive or negative). Therefore, large numbers are representative of the trend and can be used to compensate for the errors caused by caching and reduce the accumulation of cache errors. As shown in Figure 4, the *index* represents that CO is applied in the first *index* steps. The dog's tongue is repaired as the index increases. For relatively small values, we consider it to be an accumulation of positive and negative values around zero. If they are applied in the later stage of generation, they will cause problems such as blurred background details. As shown in Figure 4, when *index* = 19, the details of the water in the bird's background and the grass in the dog's background are greatly weakened. Therefore, the step at which cache optimization

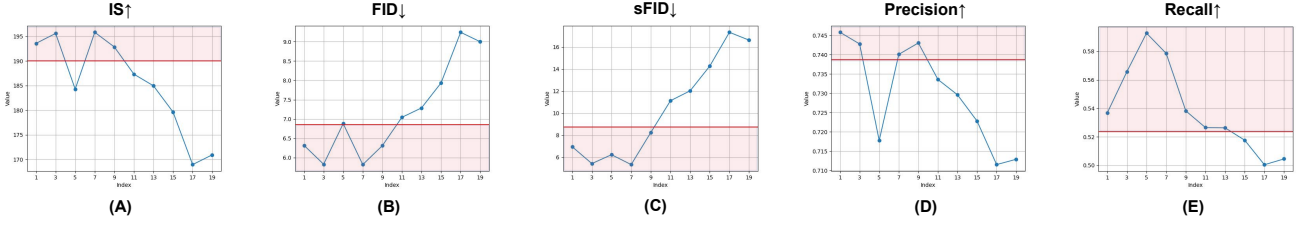


Figure 5. Effect of COD. The generation quality after performing CO on cached blocks with $t \leq index$.

is applied should be in the early stage of generation. In this way, through model operations, the noise with small absolute values will be mapped into the required generated content, thus avoiding the above-mentioned problems.

Based on the above analysis, we take the magnitude of the error \mathcal{V} and the step position $\frac{t}{\mathcal{T}}$ of caching as important judgment conditions for cache optimization determination. In response to this, we design the following formula to rank the cache optimization priorities \mathcal{P} of different blocks:

$$\mathcal{P}_{(t,l)} = \delta \cdot (\gamma \cdot \mathcal{V}_{(t,l)} + (1 - \gamma) \cdot \frac{\mathcal{T} - t}{\mathcal{T}}), \quad (6)$$

in which γ represents a regulation coefficient, which is used to adjust the importance of the error and step positions. When the l -th block at the t -th step is cached, $\delta = 1$; otherwise, $\delta = 0$. And we do not distinguish between the Attention layers and the MLP layers, as they make the same contribution to the calculation of \mathcal{V} . We set a threshold \mathcal{H} , which is used to adjust the level of cache optimization. When $\mathcal{P}_{(t,l)} > \mathcal{H}$, we perform cache optimization on the l -th block at the t -th step.

Cache Optimization. After completing the cache optimization determination and deciding that a certain block requires cache optimization, we need to consider how to appropriately embed the “trend” ($\mathcal{E}_{\text{Attn}}$ and \mathcal{E}_{MLP}) from the prior knowledge into the sampling process to reduce cache errors. Since the original intention of caching is to reduce the time consumption of sampling, embedding the “trend” can only involve a minimal amount of computation. Additionally, the “trend” only contains the common information of a certain model’s generation, while the generation also depends on the input class or prompt. Therefore, it is necessary to map the “trend” to the features in the generation process, fuse them together, and then offset the errors caused by caching.

Regarding the issue of time consumption, the prior knowledge used in this work is extracted in advance and does not take up the time of the sampling process. Moreover, we do not pre-process the “trend” using the process information from sampling. As for embedding the “trend”, after weighting it, we first multiply it by the cache information at the corresponding position and then add it to the sampling

process. Equation 3 can be written in the following form:

$$\begin{aligned} \mathcal{F}_{\text{Attn}} &= \mathbf{x} + \text{Ada} \circ (f_{\text{Attn}}(\mathbf{x}) \cdot (1 + \theta \cdot \mathcal{E}_{\text{Attn}})), \\ \mathcal{F}_{\text{MLP}} &= \mathbf{x} + \text{Ada} \circ (f_{\text{MLP}}(\mathbf{x}) \cdot (1 + \theta \cdot \mathcal{E}_{\text{MLP}})), \end{aligned} \quad (7)$$

in which θ represents the parameter for adjusting the magnitude of “trend”. And Ada is the abbreviation of AdaLN.

4. Experiment

In this section, we evaluate the proposed EOC method and compare it with rule-based and training-based methods. We also use ablation experiments to verify the effectiveness of the method proposed in this paper.

RQ1: How to determine if a specific block needs cache optimization?

RQ2: What kind of cache optimization should be performed?

RQ3: How does EOC compare with other methods?

4.1. Experiment Settings

In this section, we test on the 1000-class ImageNet (Deng et al., 2009) dataset. For DiT, in all experiments, we use DDIM (Song et al., 2020) for sampling with $L = 20$ steps. To evaluate generated-image quality, we use IS, FID, sFID, Precision, and Recall metrics. When comparing different caching and caching-optimization scenarios, we randomly generate 50k samples for objective evaluation at a 256×256 resolution. All calculations are done on an A40 GPU.

To conveniently demonstrate the method proposed in this paper, we default to setting $N = 2$, which means the cached features are reused at most once. And to present the methods more conveniently, we give the abbreviations of Rule-based Method (RM), Training-based Method (TM), Error-Optimized Cache (EOC), Cache Optimization Determination (COD), and Cache Optimization (CO). Among them, the data of TM is reproduced using the open-source code provided by the authors of learning-to-cache (Ma et al., 2024a). The data of RM is obtained by summarizing the experience from previous works (Selvaraju et al., 2024), where 25% or 50% of the blocks are cached.

Table 2. Comparison of cache optimization positions. (1). Apply the optimization to the Attention layers and the MLP layers respectively; (2). Apply the optimization to both the Attention layers and the MLP layers simultaneously.

Method	Caching level	CO Strategy	IS \uparrow	FID \downarrow	sFID \downarrow	Precision \uparrow	Recall \uparrow
RM	25%	N/A	220.011	3.870	5.185	0.783	0.569
		Attn+MLP	218.363	3.692	5.122	0.781	0.585
		MLP	207.959	4.373	6.019	0.758	0.601
		Attn	207.425	5.597	11.148	0.764	0.519
TM	22%	N/A	225.004	3.539	4.710	0.788	0.563
		Attn+MLP	223.957	3.451	4.675	0.789	0.570
		MLP	218.314	3.725	5.404	0.777	0.588
		Attn	224.705	3.909	5.645	0.792	0.543

Table 3. Comparison of cache embedding methods. Comparing the effects of using addition and multiplication to embed Prior Knowledge.

CO Strategy	Caching level	IS \uparrow	FID \downarrow	sFID \downarrow	Precision \uparrow	Recall \uparrow
No Cache	0	223.490	3.484	4.892	0.788	0.571
RM	25%	220.011	3.870	5.185	0.783	0.569
RM-“x”		218.363	3.692	5.122	0.781	0.585
RM-“+”		218.809	3.900	5.18	0.781	0.559

4.2. Cache Optimization Determination

Effect of COD (RQ1). Regarding cache-optimization determination of which step positions to prioritize for cache optimization, we design an experiment as shown in Figure 5. This figure has five sub-graphs (A)-(E), representing IS, FID, sFID, Precision, and Recall respectively. To establish a base model, we apply a 50% Rule-based Method (RM) caching strategy to DiT. Specifically, all odd-numbered steps with $t \in \{1, 3, \dots, 19\}$ were cached. The value of this base model is represented by the red horizontal line in each graph. The abscissa index of the ten blue dots in the figure represents cache optimization is performed on steps where $t \leq index$.

Through observation, we can find that if we perform cache optimization on all cache positions ($index = 19$), cache optimization will have a significant negative impact on the model’s generation. As the value of $index$ gradually decreases, the model’s generation performance gradually improves. When $index \in \{7, 9\}$, the model outperforms the base model in every evaluation criterion, and the effect of cache optimization is the best at this time. Therefore, we should try our best to avoid performing cache optimization on blocks with later steps.

4.3. Cache optimization

Implementation of CO (RQ2). To demonstrate the necessity and effectiveness of each implementation detail in cache optimization, we design the following three experiments. We compare the impacts of different cache optimization positions, different cache embedding methods, and different cache hyperparameters on the generation quality.

Previous caching methods focused on Attention and MLP layers. To explore what to optimize in cached content, we study cache-optimization application locations. Table 2 shows that when cache optimization is applied to both Attention and MLP layers simultaneously, the best generation quality can be achieved (FID: 3.870 to 3.692 for RM, 3.539 to 3.451 for TM). But applying cache optimization to only one of them significantly reduces generation quality, sometimes even worse than no optimization. So, synchronously optimizing both layers is crucial for leveraging this method’s advantages.

Regarding the selection of the mapping method for prior knowledge, by observing Table 3, we can find that by using the multiplication method in Equation 7 to map the prior knowledge to the data distribution of the generation process can better reduce the cache error. As for methods that directly add “trend” to the generation process, experiments show that regardless of the value of θ , the generation quality (experiment will be placed in the appendix) will only be worse than or infinitely close to the situation without cache optimization. Therefore, embedding cache optimization using the addition method actually introduces noise.

Finally, regarding the selection of the mapping threshold for prior knowledge, we present Table 4. It can be found that the RM and TM methods achieve the most balanced generation results when $\theta = 0.01$ and $\theta = 0.005$ respectively (The full experiment will be placed in the appendix). For this difference, we believe that because the TM method contains additional training information, there will be a certain deviation between the generation process and the original model, causing the θ value of TM to be smaller.

Table 4. Definition of θ : Comparing the generation quality obtained with different values of θ under the RM and TM methods.

Method	Weight(θ)	IS \uparrow	FID \downarrow	sFID \downarrow	Precision \uparrow	Recall \uparrow
RM+EOC	N/A	220.011	3.870	5.185	0.783	0.569
	0.02	211.368	3.892	5.402	0.765	0.602
	0.012	215.595	3.768	4.975	0.772	0.589
	0.01	218.363	3.692	5.122	0.781	0.585
	0.008	217.656	3.706	4.936	0.776	0.584
	0.005	218.263	3.765	5.137	0.779	0.569
TM+EOC	N/A	225.004	3.539	4.710	0.788	0.563
	0.01	223.062	3.473	4.904	0.786	0.580
	0.006	223.489	3.447	4.696	0.788	0.575
	0.005	223.957	3.451	4.675	0.789	0.570
	0.004	224.248	3.460	4.663	0.789	0.568
	0.003	225.030	3.476	4.659	0.788	0.569

Table 5. Effect of EOC: Comparing the generation quality of RM and TM before and after applying EOC. And RM includes two scenarios: normal-intensity caching (25%) and over-caching (50%).

Cache Strategy	Caching level	IS \uparrow	FID \downarrow	sFID \downarrow	Precision \uparrow	Recall \uparrow
N/A	0	223.490	3.484	4.892	0.788	0.571
RM	25%	220.011	3.870	5.185	0.783	0.569
	50%	190.046	6.857	8.757	0.739	0.524
RM+EOC	25%	218.363	3.692	5.122	0.781	0.585
	50%	195.844	5.821	5.342	0.740	0.579
TM	22%	225.004	3.539	4.710	0.788	0.563
TM+EOC	22%	223.957	3.451	4.675	0.789	0.570

4.4. Comparison with Other Methods

Effect of EOC (RQ3). After verifying the effectiveness and necessity of each part of EOC, we apply EOC to RM and TM with different caching intensities (25% and 50%) and compare the changes in generation quality before and after the application. As shown in Table 5, compare with the original methods RM and TM, the methods using EOC perform better on more parameters (bolded values). Specifically, for RM+EOC, the FID values of the models with two caching intensities decrease from 3.870 and 6.857 to 3.692 and 5.821. The sFID values decrease from 5.185 and 8.757 to 5.122 and 5.342. For TM+EOC, the model performs better in all metrics except IS. We believe that the reason for the decrease in IS is that there is still a small amount of noise in the prior knowledge that has not been fully mapped to the features of the generation process.

Finally, we also need to compare the changes in the generation time before and after adding EOC. As shown in Table 6, after using EOC, the time consumption of RM and TM only increased by about 0.56% and 0.22% respectively. Comparing this cost with the 4.60% and 2.49% reduction in FID, it is worthwhile and acceptable.

Table 6. Compare the changes in the computational load for generating eight images before and after cache optimization.

Cache Strategy	FID \downarrow	latency(s) \downarrow
RM	3.870	2.664 \pm 0.023
RM+EOC	3.692	2.679 \pm 0.056
TM	3.539	2.707 \pm 0.026
TM+EOC	3.451	2.713 \pm 0.013

5. Conclusion

In this paper, we propose EOC, an Error-Optimized Cache method for the Diffusion Transformer (DiT). Our work extracts prior information from the DiT generation process and uses it to determine whether the cached blocks need cache optimization. Finally, we embed the variation of the prior information into the caching process, effectively reducing caching errors and preventing error accumulation. The proposed EOC can generate samples of higher quality with little increase in computational cost. Through model comparison and ablation experiments, we achieve better performance under RM and TM with different caching intensities, which also verifies the effectiveness and necessity of the innovations we proposed.

We find that the addition of EOC has a slight negative impact on some parameters (such as IS). Therefore, we subsequently plan to investigate the embedding method for noise screening and cache optimization.

Impact Statement

This paper aims to reduce the error accumulation caused by the caching in DiT, which is closely related to generating high-quality content. We hope that our research will contribute to reducing the time required for content generation and facilitate the development of AI systems that are beneficial to society.

References

- Achiam, J., Adler, S., Agarwal, S., Ahmad, L., Akkaya, I., Aleman, F. L., Almeida, D., Altenschmidt, J., Altman, S., Anadkat, S., et al. Gpt-4 technical report. *arXiv preprint arXiv:2303.08774*, 2023.
- Bhargat, Y., Lee, J., Nagel, M., Blankevoort, T., and Kwak, N. Lsq+: Improving low-bit quantization through learnable offsets and better initialization. In *Proceedings of the IEEE/CVF conference on computer vision and pattern recognition workshops*, pp. 696–697, 2020.
- Castells, T., Song, H.-K., Kim, B.-K., and Choi, S. Ld-pruner: Efficient pruning of latent diffusion models using task-agnostic insights. In *Proceedings of the IEEE/CVF Conference on Computer Vision and Pattern Recognition*, pp. 821–830, 2024.
- Chen, P., Shen, M., Ye, P., Cao, J., Tu, C., Bouganis, C.-S., Zhao, Y., and Chen, T. $\Delta - dit$: A training-free acceleration method tailored for diffusion transformers. *arXiv preprint arXiv:2406.01125*, 2024.
- Deng, J., Dong, W., Socher, R., Li, L.-J., Li, K., and Fei-Fei, L. Imagenet: A large-scale hierarchical image database. In *2009 IEEE conference on computer vision and pattern recognition*, pp. 248–255. Ieee, 2009.
- Dong, X., Chen, S., and Pan, S. Learning to prune deep neural networks via layer-wise optimal brain surgeon. *Advances in neural information processing systems*, 30, 2017.
- Guo, D., Rush, A. M., and Kim, Y. Parameter-efficient transfer learning with diff pruning. *arXiv preprint arXiv:2012.07463*, 2020.
- Guo, Y., Wang, C., Yu, S. X., McKenna, F., and Law, K. H. Adaln: a vision transformer for multidomain learning and predisaster building information extraction from images. *Journal of Computing in Civil Engineering*, 36(5): 04022024, 2022.
- Ho, J., Jain, A., and Abbeel, P. Denoising diffusion probabilistic models. *Advances in neural information processing systems*, 33:6840–6851, 2020.
- Lee, N., Ajanthan, T., Gould, S., and Torr, P. H. A signal propagation perspective for pruning neural networks at initialization. *arXiv preprint arXiv:1906.06307*, 2019.
- Li, S., Hu, T., Khan, F. S., Li, L., Yang, S., Wang, Y., Cheng, M.-M., and Yang, J. Faster diffusion: Rethinking the role of unet encoder in diffusion models. *CoRR*, 2023a.
- Li, X., Liu, Y., Lian, L., Yang, H., Dong, Z., Kang, D., Zhang, S., and Keutzer, K. Q-diffusion: Quantizing diffusion models. In *Proceedings of the IEEE/CVF International Conference on Computer Vision*, pp. 17535–17545, 2023b.
- Li, Y., Gong, R., Tan, X., Yang, Y., Hu, P., Zhang, Q., Yu, F., Wang, W., and Gu, S. Brecq: Pushing the limit of post-training quantization by block reconstruction. *arXiv preprint arXiv:2102.05426*, 2021.
- Liu, L., Zhang, S., Kuang, Z., Zhou, A., Xue, J.-H., Wang, X., Chen, Y., Yang, W., Liao, Q., and Zhang, W. Group fisher pruning for practical network compression. In *International Conference on Machine Learning*, pp. 7021–7032. PMLR, 2021.
- Liu, Z., Sun, M., Zhou, T., Huang, G., and Darrell, T. Rethinking the value of network pruning. *arXiv preprint arXiv:1810.05270*, 2018.
- Lu, C., Zhou, Y., Bao, F., Chen, J., Li, C., and Zhu, J. Dpm-solver: A fast ode solver for diffusion probabilistic model sampling in around 10 steps. *Advances in Neural Information Processing Systems*, 35:5775–5787, 2022.
- Luhman, E. and Luhman, T. Knowledge distillation in iterative generative models for improved sampling speed. *arXiv preprint arXiv:2101.02388*, 2021.
- Ma, X., Fang, G., Mi, M. B., and Wang, X. Learning-to-cache: Accelerating diffusion transformer via layer caching. *arXiv preprint arXiv:2406.01733*, 2024a.
- Ma, X., Fang, G., and Wang, X. Deepcache: Accelerating diffusion models for free. In *Proceedings of the IEEE/CVF Conference on Computer Vision and Pattern Recognition*, pp. 15762–15772, 2024b.
- Meng, C., Rombach, R., Gao, R., Kingma, D., Ermon, S., Ho, J., and Salimans, T. On distillation of guided diffusion models. In *Proceedings of the IEEE/CVF Conference on Computer Vision and Pattern Recognition*, pp. 14297–14306, 2023.

- Meng, K., Bau, D., Andonian, A., and Belinkov, Y. Locating and editing factual associations in gpt. *Advances in Neural Information Processing Systems*, 35:17359–17372, 2022.
- Nagel, M., Amjad, R. A., Van Baalen, M., Louizos, C., and Blankevoort, T. Up or down? adaptive rounding for post-training quantization. In *International Conference on Machine Learning*, pp. 7197–7206. PMLR, 2020.
- Peebles, W. and Xie, S. Scalable diffusion models with transformers. In *Proceedings of the IEEE/CVF International Conference on Computer Vision*, pp. 4195–4205, 2023.
- Salimans, T. and Ho, J. Progressive distillation for fast sampling of diffusion models. *arXiv preprint arXiv:2202.00512*, 2022.
- Selvaraju, P., Ding, T., Chen, T., Zharkov, I., and Liang, L. Fora: Fast-forward caching in diffusion transformer acceleration. *arXiv preprint arXiv:2407.01425*, 2024.
- Shih, A., Belkhale, S., Ermon, S., Sadigh, D., and Anari, N. Parallel sampling of diffusion models. *Advances in Neural Information Processing Systems*, 36, 2024.
- So, J., Lee, J., Ahn, D., Kim, H., and Park, E. Temporal dynamic quantization for diffusion models. *Advances in Neural Information Processing Systems*, 36, 2024.
- Song, J., Meng, C., and Ermon, S. Denoising diffusion implicit models. *arXiv preprint arXiv:2010.02502*, 2020.
- Song, Y., Dhariwal, P., Chen, M., and Sutskever, I. Consistency models. *arXiv preprint arXiv:2303.01469*, 2023.
- Wang, Y., Chen, X., Ma, X., Zhou, S., Huang, Z., Wang, Y., Yang, C., He, Y., Yu, J., Yang, P., et al. Lavie: High-quality video generation with cascaded latent diffusion models. *International Journal of Computer Vision*, pp. 1–20, 2024.
- Wimbauer, F., Wu, B., Schoenfeld, E., Dai, X., Hou, J., He, Z., Sanakoyeu, A., Zhang, P., Tsai, S., Kohler, J., et al. Cache me if you can: Accelerating diffusion models through block caching. In *Proceedings of the IEEE/CVF Conference on Computer Vision and Pattern Recognition*, pp. 6211–6220, 2024.
- Wu, J., Wang, H., Shang, Y., Shah, M., and Yan, Y. Ptq4dit: Post-training quantization for diffusion transformers. *arXiv preprint arXiv:2405.16005*, 2024.
- Xu, J., Liu, X., Wu, Y., Tong, Y., Li, Q., Ding, M., Tang, J., and Dong, Y. Imagereward: Learning and evaluating human preferences for text-to-image generation. *Advances in Neural Information Processing Systems*, 36, 2024.
- Yin, T., Gharbi, M., Zhang, R., Shechtman, E., Durand, F., Freeman, W. T., and Park, T. One-step diffusion with distribution matching distillation. In *Proceedings of the IEEE/CVF Conference on Computer Vision and Pattern Recognition*, pp. 6613–6623, 2024.
- Zhao, X., Jin, X., Wang, K., and You, Y. Real-time video generation with pyramid attention broadcast. *arXiv preprint arXiv:2408.12588*, 2024.
- Zheng, H., Nie, W., Vahdat, A., Azizzadenesheli, K., and Anandkumar, A. Fast sampling of diffusion models via operator learning. In *International conference on machine learning*, pp. 42390–42402. PMLR, 2023.